EPJ Web of Conferences **264**, 01011 (2022) https://doi.org/10.1051/epjconf/202226401011
EFM 2021

Simcenter STAR-CCM+ software for CFD and heat transfer calculations in minichannels

Norbert Dadas[1], *Artur* Piasecki[2], and *Magdalena* Piasecka[1*]

[1] Kielce University of Technology, Faculty of Mechatronics and Mechanical Engineering, al. 1000-lecia Panstwa Polskiego 7, PL-25-314 Kielce, Poland
[2] Echo Investment S.A., Al. Solidarnosci 36, 25-323 Kielce, Poland

Abstract. The paper focuses on CFD modelling and numerical simulation of heat transfer during fluid flow in minichannels. The data from the experiment were adopted into Simcenter Star-CCM+ software. The test section comprised seven or twenty-one parallel minichannels of rectangular cross sections. Each minichannel was 1 mm height. During the experimental series, the temperature measurements of the heated wall were recorded due to an infrared camera. Measurement data was compared with the results obtained from numerical calculations. Fluorinert FC-72 was used as a working fluid in experiments and simulations. An increase in the values of the heat transfer coefficient was observed for the test section with 21 minichannels compared to that with seven minichannels. Numerical simulations helped to identify how the change in the number of minichannels affects the intensification of heat transfer during flow without the time- and cost-consuming experimental tests

1 Introduction

The miniaturization of devices that generate large heat fluxes in various industries requires the search for high-performance heat exchangers, including phase change and minigeometries [1, 2]. A review of the relevant literature and selected publications covering heat transfer during cooling liquid flow in rectangular minichannels was presented in [3, 4]. The results of experiments conducted in the test section with an annular minigap are described in [5]. The review of the literature leads to the conclusion that, although much has been written recently on heat transfer during flow in minichannels, the literature does not offer any generalized conclusions concerning heat transfer during liquid flow in such miniature systems, while experiments required complicated apparatus and efforts.

CFD simulations can be used to minimize the number of experimental studies by selecting only those with a significant improvement in parameters. The model for the lifetime of the EGR coolers was proposed in [6]. CFD calculations helped simulate the temperature of the metal during the heating and cooling cycles. In [7] the 3D model of shell side flow in rod-baffle heat exchangers with spirally corrugated tubes was compared to rod-baffle heat exchangers with plain tubes. It was concluded that 10% higher heat transfer values were obtained when spirally corrugated tubes were applied in rod-baffle heat exchangers compared to plain tubes.

Preparing a correct numerical simulation can lead to many problems. Large differences between elements require appropriate mesh selection and optimization [8]. To verify the model, the results of the numerical calculations should be compared with the known values resulting from the correlation or directly obtained from the experiment. With deviations not exceeding 10%, convergence can be considered good, ensuring the credibility of the simulation [9].

2 Experimental setup

The data from experiments conducted on a research set-up with the test section comprising a group of minichannels were adopted for CFD numerical simulations. The main objective of this paper was to determine how the number of minichannels influences heat transfer during flow by analyzing the values of the heat transfer coefficient. The aim was achieved on the basis of the results from the numerical computations, obtained using the data from the experimental investigations. In the calculations, two variants of the test section that differed in the number of minichannels were applied. In one construction variant, the test section consisted of seven minichannels, while in the other 21 minichannels were tested. The side walls of the minichannels were formed within a Teflon spacer. The main elements of the test section are shown in Fig. 1. The most important information about the dimensions of the main elements of the test section is listed in Table 1.

* Corresponding author: tmpmj@tu.kielce.pl

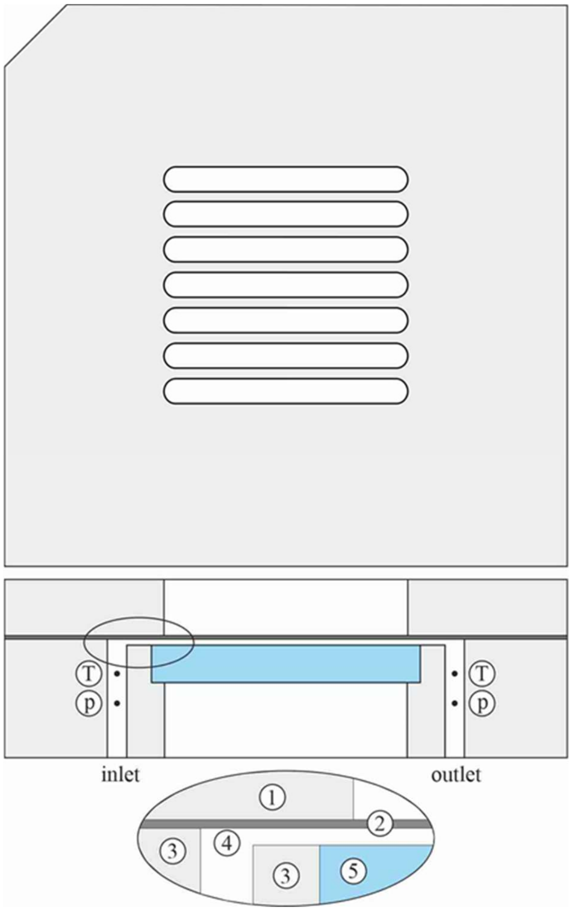

Fig. 1. Main elements of the test section, 1 – top cover, 2 – heater (heated foil), 3 – channel body, 4 – minichannel, 5 – glass panel.

Table 1. Dimensions of the main elements of the test section.

Element of the test section	Dimensions (mm) (height x length x width)
Top cover	9 x 90 x 90
Heated foil	0.1 x 90 x 40
Channel body	18 x 90 x 90
Area of minichannels	1 x 57 x 38
Single minichannel (7 channels in a group)	1 x 57 x 4
Single minichannel (21 channels in a group)	1 x 57 x 0.86
Glass panel	6 x 43 x 38

The materials of the main elements of the test section are as follows (see Fig. 1):

- 1, 3 – aluminum alloy PA6,
- 2 – Haynes-230 alloy,
- 5 – glass panel.

To perform the CFD simulation physical properties of the materials were entered into the program (Table 2). These data were required for the equations and the appropriate procedure used in the numerical computations.

Table 2. Physical properties of the materials used in the CFD calculations.

Material	Density ($kg \cdot m^{-3}$)	Dynamic viscosity ($Pa \cdot s$)	Specific heat ($J \cdot kg^{-1} \cdot K^{-1}$)	Thermal conductivity ($W \cdot m^{-1} \cdot K^{-1}$)
FC-72	1680	$6.4 \cdot 10^{-4}$	1100	0.057
Aluminum	2702	-	903	237
Haynes -230	8970	-	400	8.9÷14.4 for temperature range from 293.1 (K) to 673.1 (K)
Glass	2500	-	840	1.4
Teflon	2160	-	702	0.21

During the experimental sets, Fluorinert FC-72 was circulating as the working fluid in the main loop. One wall of the minichannels was a thin foil resistively heated. Recording the temperature on the outer surface of the heated foil was realized by infrared thermography. The reverse surface of the foil with visible two-phase fluid flow was observed through a glass panel. The temperature and pressure of the cooling fluid were measured at the inlet and outlet of the channel. There were no significant changes in the ambient air temperature; it was within the range of +/- 0.2 K throughout the measurement. The experimental parameters were captured as signals from K-type thermocouples, pressure meters, flow meter, ammeter and voltmeter. Data collected for a selected setting of the supplied heat flux, taken for the calculations, are shown in Table 3. Additionally, captured images from an infrared camera were converted to obtain a temperature distribution on the outer surface of the heater.

Table 3. The main experimental parameters.

Specified variables	
Temperature of FC-72 fluid at the minichannel inlet (K)	286.05
Temperature of ambient air (K)	294.45
Atmospheric pressure (kPa)	95.47
Overpressure at the minichannel inlet (kPa)	93.01
Overpressure at the minichannel outlet (kPa)	94.17
Mass flow rate (kg/h)	21.99
Heat flux supplied to the heater (W)	94.79

3 Numerical calculations

Numerical calculations were provided in Simcenter Star-CCM+ software, version 2020.2.1 Build 15.04.010. The elements of the 3D model were meshed using a polyhedral grid. The number of cells, faces, and vertices of the individual elements is presented in Table 4.

Table 4. Data of meshed regions.

Region	Cells	Faces	Vertices
Top cover	1 998 550	9 565 776	6 498 512
Heater	6 127 213	26 059 982	16 858 042
Channel body	597 633	2 871 269	1 957 548
Top spacer	4 826 177	20 313 609	12 328 173
Bottom spacer	3 864 620	17 093 891	10 888 766
Glass panel	143 079	661 636	438 453
Fluid FC-72	1 587 691	7 007 002	4 457 513

Due to the large differences in the thickness of the elements, the mesh had additional prism layers implemented. This option allowed for significantly densification of the mesh at the points of contact between elements, increasing the quality of the calculations. Several versions of the meshes were tested. It was assumed that a precise mesh selection significantly affects the quality of the results. The residuals were flattened out after 6000 iterations, but to be sure of the correctness of the numerical calculations, they were proceeded to 7500. The absolute errors in the solutions of particular variables ranged from 10^{-6} (energy) to 10^{-13} (turbulent dissipation rate) and the continuity was about 10^{-8}.

Mesh dependency studies based on GCI were carried out to estimate the numerical accuracy resulting from mesh resolution. To define the accuracy discretization error, the model was meshed with three grids with different sizes to obtain a range of 3 to 15 million cells. The results were widely discussed in [10].

Table 5 presents the general assumptions adopted for the two continua: the fluid, Fluorinert FC-72, and the solid, a heater (a thin heated foil) made of Haynes-230 alloy. The rest of the solid continua was similar in assumptions to the heater.

Table 5. The general assumptions adopted for the fluid and the solid in the calculations by Simcenter Star-CCM+ software.

Continua	General assumptions
Fluid: Fluorinert FC-72	Circumferential heat flux averaging
	Constant density
	Gradients
	Gravity
	Implicit unsteady
	K-epsilon turbulence
	Liquid
	Realizable k-epsilon two-layer
	Reynolds-averaged Navier-Stokes
	Segregated flow
	Segregated fluid temperature
	Solution interpolation
	Three dimensional
	Turbulent
	Two-layer all y+ wall treatment
	Wall distance
Solid: Haynes-230 alloy	Constant density
	Gradients
	Implicit unsteady
	Segregated solid energy
	Solid
	Solution interpolation
	Three dimensional

4 Results

The data from the experimental set (see Table 2) were entered into the Simcenter Star-CCM+ numerical program and the general assumptions adopted for the fluid Fluorinert FC-72 and the heater made of Haynes-230 (see Table 5) were made. After computations, the temperature of the outer heated foil surface was compared with that recorded by an infrared camera during the experiment. The temperature on the outer heated surface versus distance from the minichannel inlet, obtained from the experiment with seven minichannels on the basis of IR measurement and from numerical computations due to Simcenter Star-CCM +, are given in Fig. 2.

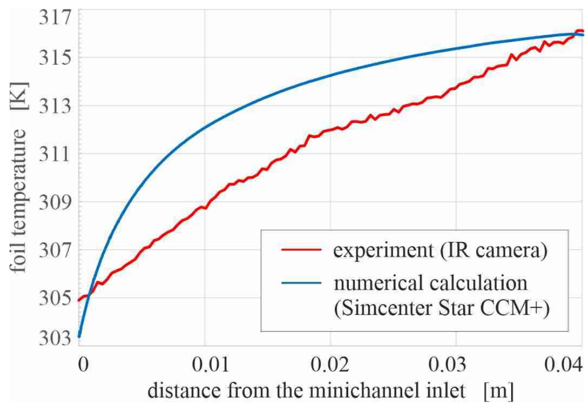

Fig. 2. Temperature on the outer heated surface versus distance from the minichannel inlet, obtained from the experiment with seven minichannels on the basis of IR measurement and from numerical computations due to Simcenter Star-CCM+.

When analyzing the results shown in Fig. 2 it is observed that the highest temperature difference between the results of the experiment and the numerical calculation reached 3 K. It can be underlined that the accuracy of the infrared camera is about 2 K. Furthermore, the values of the temperatures at the ends of the minichannel are very similar. The assumptions introduced into the numerical program regarding the heat exchange between the test section and the environment might result in even better compliance of both temperature dependences.

After numerical calculations and validation of the results gained for the test section with seven minichannels (carried out as a comparison between the foil temperature values obtained from the experiment and the numerical calculation), the number of minichannels was greatly increased.

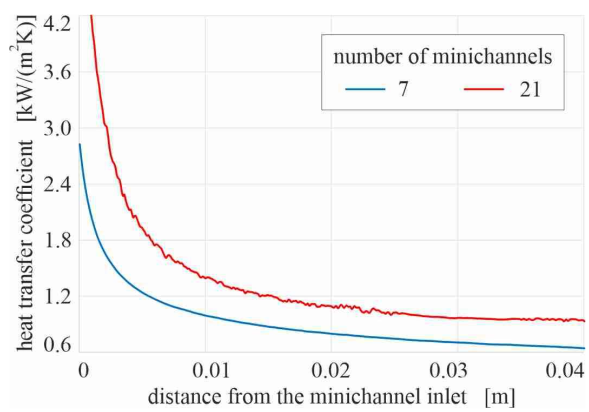

Fig. 3. Heat transfer coefficient versus distance from the minichannel inlet obtained from numerical computations due to Simcenter Star-CCM+ software; the results for seven and 21 minichannels.

https://doi.org/10.1051/epjconf/202226401011

The experimental data listed in Table 3 were used in the numerical calculations for the test section comprising 21 channels. The heat transfer coefficient (HTC) versus distance from the minichannel inlet is illustrated in Fig. 3. The HTC values determined for the test section with seven minichannels are also presented in this figure.

When analyzing the dependences shown in Fig. 3, it can be noticed that the increase in the number of minichannels in the test section results in a 30% higher HTC. Changing the number of minichannels in the test section also affects the fluid pressure and velocity in each of the channels. Furthermore, these parameters also affect the values of the temperature and the heat transfer coefficient.

Figure 4 shows the distributions of temperature (Fig. 4a), absolute pressure (Fig. 4b), and velocity (Fig. 4c) obtained from numerical computations. The data refer to the longitudinal cross section of the central minichannel, whereas the test section with seven channels was assumed in the calculations.

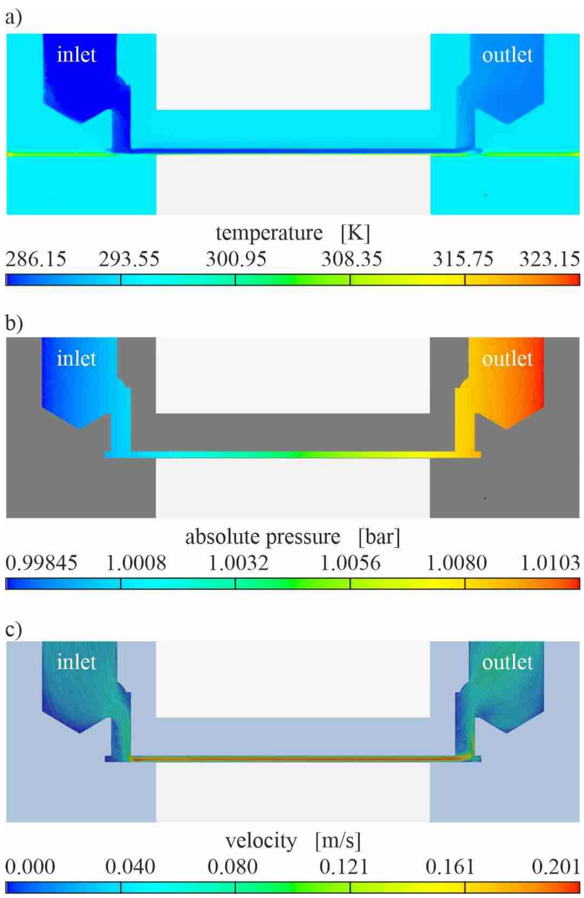

Fig. 4. Results from the numerical calculations obtained in the longitudinal cross section of the central minichannel showing the distributions of: a) temperature, b) fluid absolute pressure and c) fluid velocity; screenshots from Simcenter STAR-CCM + software.

5 Conclusions

The main aim of this paper was to present CFD modelling and numerical computations concerning boiling heat transfer during fluid flow in minichannels. For this purpose, the selected experimental data were adopted for numerical calculations. The calculations were performed using Simcenter Star-CCM+ software. The experimental data were used to validate the numerical results. Data from the numerical computations collected for the test section with seven minichannels were compared with the heater temperature experimentally measured. In further numerical simulations, the number of minichannels was increased to 21. Such calculations helped determine how the change in the number of minichannels affects the intensification of heat transfer during flow.

The authors noted the following comments and observations:

- Increasing the number of minichannels in the test section causes increasing obtained heat transfer coefficient values (up to 30%);
- Validation of the experiment with numerical simulations ensures that physical models and grid convergence enable acquired the reliable results;
- CFD simulations helped to identify how the change in the number of minichannels affects the intensification of heat transfer during flow without the time- and cost-consuming experimental tests.

Acknowledgments

The research reported herein was supported by a grant from the National Science Centre, Poland, No. UMO-2018/31/B/ST8/01199.

The calculations were made using the Simcenter Star-CCM+ software developed by Siemens PLM Software Inc., provided by GMSystem which is a supplier of Siemens Digital Industries Software in Poland.

References

1. M. Klugmann, P. Dąbrowski, D. Mikielewicz, Appl. Therm. Eng. **181** (2020)
2. R. Kaniowski, R. Pastuszko, EPJ Web Conf. **180**, No. 02041 (2018)
3. B. Maciejewska, M. Piasecka, A. Piasecki, Heat Transf. Eng. **43** (2021)
4. M. Piasecka, B. Maciejewska, P. Łabędzki, Energies **13** No. 6647 (2020)
5. M. Piasecka, T. Musiał, A. Piasecki, EPJ Web Conf. **213** No. 02066 (2019)
6. B.G. Holland, T.L. McKinley, B.R. Storkman, SAE Int. J. Engines **8** (2015)
7. J.J. Liu, Z.C. Liu, W. Liu, Int. J. Therm. Sci. **89** (2014)
8. J. Wajs, T. Kura, D. Mikielewicz, E. Fornalik-Wajs, J. Mikielewicz, Energy **238** (2022)
9. P. Dąbrowski, R. Kumar, Int. Commun. Heat Mass Transf. **129** (2021)
10. M. Piasecka, A. Piasecki, N. Dadas, Energies **15** No. 536 (2022)